Geophys. J. R. astr. Soc. (1970) **19**, 237–260.

Separation of Magnetic Variation Fields and Conductive Structures in the Western United States

H. Porath, D. W. Oldenburg and D. I. Gough

Summary

The variation field of a polar substorm was recorded by an array of 42 variometers in the western United States. This field has been separated by surface integral methods into parts of external and internal origins, at four times in the time domain and at four periods in the period domain. It is shown that the anomalies in the vertical and east–west horizontal variation fields are of internal origin and that the external fields vary smoothly over the array. The separated fields in both domains show internal currents induced in north–south striking conductive structures by the east–west horizontal field. Phase differences between the normal and anomalous fields are about 30°, and indicate large, highly-conducting structures in which self-induction controls the currents. The in-phase normalized anomalous fields at period 89 minutes have been approximated by two-dimensional models made up of upheavals of semi-circular section and a step in the surface of a perfectly-conducting half-space. A semi-circular upheaval of radius 150 km from an unperturbed level at depth 360 km models the anomaly related to the Southern Rockies. A step of height 120 km at the Wasatch Front, together with a semi-cylinder of radius 100 km under the Wasatch fault belt, give a good approximation to the observed anomaly at the Wasatch Front. The actual structures may be somewhat shallower and smoother. The real conductivity is estimated at $2 \cdot 10^{-12}$ e.m.u., a value which would be expected at temperatures near 1500 °C. Such temperatures are reasonable at the depths concerned.

1. Introduction

Geomagnetic variations measured at the surface of the Earth consist of an external part originating in currents in the ionosphere and magnetosphere, and an internal part arising from currents induced by the external part in the conductive regions in the upper few hundred kilometres of the Earth. Anomalies in the field at the surface arise from lateral conductivity variations in the crust and upper mantle. Quantitative interpretation of such conductive structures requires the separation of the internal and external parts of the field. The amplitude and phase relationships between the internal and external parts can then be fitted by appropriate conductivity models.

It is a result of potential theory that a field whose potential and normal component are known over a closed surface can be separated into parts of external and internal origins (Chapman & Bartels 1940). In geomagnetic deep sounding, three components of the variation field are measured and the potential can be found from

the horizontal components, though over a limited area. Rigorous separation of the fields has rarely been carried out in such studies, mainly because an insufficient number of instruments have been available to map the variation anomalies adequately. It was the purpose of the design of an inexpensive variometer by Gough & Reitzel (1967) which could be built in large numbers, to attempt separation of fields recorded simultaneously over an anomalous area. Some 42 of these variometers are now in use by the University of Alberta and the University of Texas at Dallas in a study of the crustal and upper mantle conductive structures in the western United States.

Variation anomalies found during the summer of 1967 have been described, with a qualitative interpretation, in a previous paper (Reitzel *et al.* 1970). This paper presents the results of a separation of the field of a polar substorm of 1967 September 1, and a preliminary interpretation by simple conductivity models of the relation between the separated fields. The disposition of the variometer array, and variograms of the substorm of September 1, are shown in Figs 1 and 2 of Reitzel *et al.* and are not repeated here.

2. Principles of separation

For local conductivity anomalies we can ignore the sphericity of the Earth and use a plane approximation. On a plane, fields with scale lengths large compared with the variometer array cannot be separated. Such fields will in general include an external part and a 'normal' internal part originating from the general mantle conductivity. A model of the external field of a substorm would be useful in estimating the external and normal internal parts. Rikitake (1950) has proposed an expansion of a bay variation field in associated Legendre functions of the second type, for stations at latitudes less than 45°, which may be used in this way. However, most observatories are in regions of anomalous variations, so that the validity of this analysis is somewhat uncertain. The procedures followed in the present work, with regard to removal of the inseparable field, are discussed in the next section.

Separation of fields on a plane can be achieved by approximating the horizontal and vertical components by two-dimensional Fourier series, in a manner analogous to the use of spherical harmonics for the daily variation field (Chapman & Bartels 1940). The Fourier coefficients of the external and internal fields can be obtained as described by Wiese (1965), and recombined to give maps of internal and external fields. This method implies periodic repetition of the field outside the array. Almost any reasonable assumed extrapolation should give smaller errors in the separated fields near the edges of the array. Methods of separation based on surface integrals derived from Green's theorems are, therefore, usually better for separation of local variation anomalies. Various integrals have been given by Vestine (1941), Siebert & Kertz (1957), Price & Wilkins (1963), Hartmann (1963) and Weaver (1963). In this paper we use integral formulae derived by Hartmann (1963) from Green's theorem, and also by Weaver (1963) from two-dimensional Fourier integrals. These integrals are:

$$\left.\begin{aligned} 2\pi(Z_e - Z_i)|_0 &= \int_{-\infty}^{\infty}\int \frac{(x-x_0)\,X(x,y)+(y-y_0)\,Y(x,y)}{[(x-x_0)^2+(y-y_0)^2]^{\frac{3}{2}}}\,dx\,dy \\ 2\pi(Y_e - Y_i)|_0 &= -\int_{-\infty}^{\infty}\int \frac{(y-y_0)\,Z(x,y)\,dx\,dy}{[(x-x_0)^2+(y-y_0)^2]^{\frac{3}{2}}} \\ 2\pi(X_e - X_i)|_0 &= -\int_{-\infty}^{\infty}\int \frac{(x-x_0)\,Z(x,y)\,dx\,dy}{[(x-x_0)^2+(y-y_0)^2]^{\frac{3}{2}}} \end{aligned}\right\} \quad (1)$$

The integral for separation of Z is expressed in terms of two horizontal components without intermediate determination of the potential. The point at which separation is made is (x_0, y_0). Together with the observed $Z = Z_e + Z_i$ the first formula gives Z_e and Z_i, and similarly for the other components. The surface integration can be performed in Cartesian or in polar co-ordinates, though the latter are preferable as the convergence can be tested by comparing the contributions of successive ring elements of increasing radius. An integral formula given by Price & Wilkins (1963) for $(Z_e - Z_i)$ in terms of one horizontal component only is divergent at the origin (Schmucker—personal communication) but convergence is secured by the use of both components as in (1). The contribution of a small circle of radius a at (x_0, y_0) is

$$+\pi a \left(\frac{\partial X}{\partial x}\bigg|_0 + \frac{\partial Y}{\partial y}\bigg|_0 \right) \quad \text{to} \quad 2\pi(Z_e - Z_i)|_0,$$

$$-\pi a \frac{\partial Z}{\partial y}\bigg|_0 \quad \text{to} \quad 2\pi(Y_e - Y_i)|_0, \tag{2}$$

and

$$-\pi a \frac{\partial Z}{\partial x}\bigg|_0 \quad \text{to} \quad 2\pi(X_e - X_i)|_0$$

in polar co-ordinates. In Cartesian co-ordinates the corresponding contributions of a small square of side $2a$ at the separation point are

$$2a \ln\left(\frac{\sqrt{2}+1}{\sqrt{2}-1}\right)\left[\frac{\partial X}{\partial x}\bigg|_0 + \frac{\partial Y}{\partial y}\bigg|_0\right]$$

$$-2a \ln\left(\frac{\sqrt{2}+1}{\sqrt{2}-1}\right)\left[\frac{\partial Z}{\partial y}\bigg|_0\right] \tag{3}$$

and

$$-2a \ln\left(\frac{\sqrt{2}+1}{\sqrt{2}-1}\right)\left[\frac{\partial Z}{\partial x}\bigg|_0\right].$$

The first step in a separation analysis is the interpolation of the three field components between stations and construction of contour maps. These maps can be drawn for selected instants in the time domain, or for selected periods in the period domain. In the latter case the sine and cosine Fourier transforms are mapped, so that two contour maps must be drawn for each component. One separation in the period domain gives phase and amplitude information derived from the whole variation event; in the time domain, this would require separation at many instants. Separation in the time domain can be useful, however, in revealing the instantaneous configuration of internal currents.

Interpolation and extrapolation of the horizontal components can be improved by use of the requirement that the field has a potential. The map so drawn will show a field to which the first integral formula of (1) can be applied. The potential condition can be met either by drawing contours of the horizontal components in such a way that the gradients $\partial X/\partial y = \partial Y/\partial x$ (curl-free condition) or by a relaxation of the residuals of line integrals of the horizontal components round individual squares of a grid (Price & Wilkins 1963).

3. Separation procedures

The substorm field of 1967 September 1 has been separated at four times in the time domain and at four periods in the period domain. In the time domain the instantaneous fields at 06·30, 06·45, 07·00 and 07·15 U.T. relative to their values at 05·00 U.T. were chosen.

In the period domain, the cosine and sine Fourier transforms should be separated for periods at which the spectra of the horizontal variations show large amplitudes, corresponding to high energy of the incident variation. For the substorm of September 1 the selection of periods for separation on this criterion is made difficult by differential shifts between stations of the peaks in the amplitude spectra (Fig. 1). A short-period peak occurs at period 32·5 minutes at all stations. The major energy maxima are, however, close to periods 50 minutes and 80–100 minutes. Comparison of the spectra of H and D at stations near the west and east limits of the array shows a shift of these two peaks to shorter periods for D and to longer periods for H, going from east to west. The shifts are probably source effects. Periods of 50, 60 and 89 minutes were chosen for separation as having good amplitudes of the horizontal field components. In spite of the much lower amplitude at period 32·5 minutes, the field components were separated at this period in addition, to extend the range of periods covered.

A rectangular co-ordinate system was superposed on an equal-area map of the array with the x axis northward and parallel to 108° W longitude, and the y axis eastward at this longitude. For each station axes were rotated through the small angles required by the map projection, to give the horizontal components in this co-ordinate system for the times and periods chosen for separation. Contour maps were drawn of all three components, in the time domain, of the instantaneous component value relative to that at 05·00 U.T., and in the period domain of the sine and cosine transforms on separate maps, with initial time 05·00 U.T. The contours were first linearly interpolated. For the horizontal components the interpolation was then improved by adjusting the contours to satisfy the curl-free condition, $\partial X/\partial y = \partial Y/\partial x$, as nearly as possible.

To obtain better estimates of the separation integrals within the array, the contours were extrapolated for 300 km outside the array, again with the use of the condition that the field has zero curl. Such extrapolations are naturally doubtful, but are certainly better than setting the fields outside the array equal to zero or some other constant value.

For the separations in the time domain and for those in the period domain at period 60 minutes, the surface integrals (1) were approximated in Cartesian co-ordinates by summing the contributions of squares of side 100 km. In the square centred at the point of separation, the mean gradients $\partial X/\partial x$, $\partial Y/\partial y$, $\partial Z/\partial x$ and

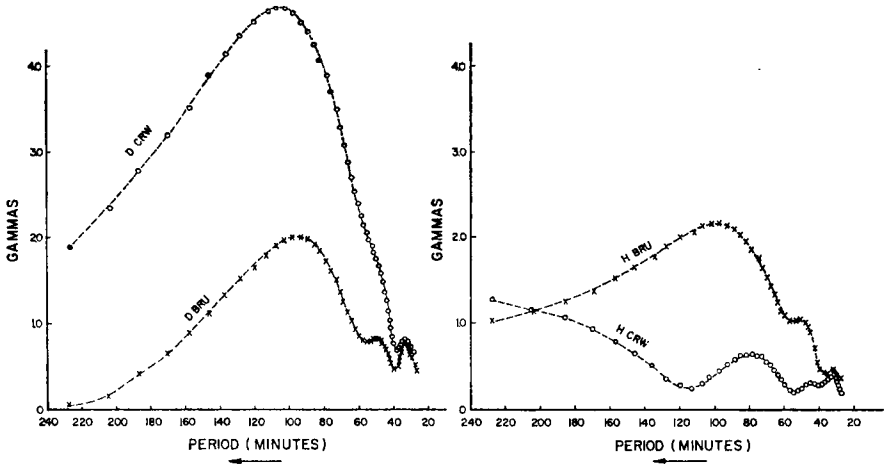

FIG. 1. Spectra of D and H components of substorm at eastern (CRW) and western (BRU) stations of Line 1.

$\partial Z/\partial y$ were estimated for use in (3); in other squares the mean values of X, Y and Z were used in (1). The antisymmetric form of the integrals (1) requires summation over an area symmetrical about the point of separation. A square of side 700 km was used as a 'summation window' centred at each point of separation. Hence in attempting separation at a point near an edge of the array, extrapolated parts of the contour map contributed much of the integral and some parts of the array area had to be excluded. Considerable errors from these edge effects will affect separations near the limits of the array. One separation in the time domain was repeated with summation windows 900×900 and 1100×1100 km. The maps of separated fields with summation windows of sides 700, 900 and 1100 km were not significantly different. This indicates that contributions from outside the 700 km summation window have little effect upon differences within the mapped area. Such contributions are indeterminate and because of them the zero level of each separated field component is unknown. For the same reason the apparent ratio of external to internal parts has no special significance.

For the separations in the period domain at periods 32·5, 50 and 89 minutes, the map was divided into squares of side 50 km and the surface integrals were computed in polar co-ordinates. In this case the programme included transformation of the square grid into a polar grid with $\Delta\theta = 11{\cdot}25°$ and $\Delta r = 50$ km. Estimates of the field gradients in the central circle were used in (2), and estimates of the field values in the annular sector areas were used in (1). The summation window in this case was a circle of radius 450 km.

As has been remarked, fields with scale lengths much larger than the dimensions of the array cannot be separated. It is therefore customary to remove from the data, before separation, a 'normal' horizontal field H_n which is assumed to be the sum of the external part H_{en} and an internal part H_{in} due to the general highly-conducting mantle at depth. In essence the removal of H_n leaves zero fields over the rest of the infinite plane over which the integrations (1) should be performed. The removal of H_n leaves an anomalous internal field, H_{ia}, to be separated from an inhomogeneous residual external field H_{ea}. Because of the large size of our array and because of the complexity of the source currents in the substorm of 1967 September 1, the normal field varies considerably between stations and cannot be approximated by a constant. An attempt was made to remove the normal field by fitting a polynomial in x and y by least squares to the horizontal components X and Y with the boundary condition $\partial X/\partial y = \partial Y/\partial x$. However, the matrix for calculating the coefficients becomes ill-conditioned for surfaces of higher order than a plane. A plane approximation can be used only after examination of the separated external field shows it to be appropriate. The procedure followed in the present work has been to make the separation analysis first. For the model studies, an estimated normal internal field, of form deduced from the separated external field, was then deducted from the separated internal field. This permitted isolation and normalization of the internal anomalous fields.

4. Separated fields in the time domain

Fig. 2 shows contoured maps of Z, X and Y at 06·30 U.T. relative to 05·00 U.T. The maps of the northward and eastward components, X and Y, have been superposed to illustrate the way in which approximately curl-free fields were contoured, and the extent to which this was achieved. These maps are typical of those used in the time-domain separations. Anomalies related to currents running roughly north–south under the Southern Rocky Mountains and the Wasatch Front form prominent features. Separated components are shown in Fig. 3. The X component shows no features of special interest in the internal field because of the north–south strike of the conductive structures.

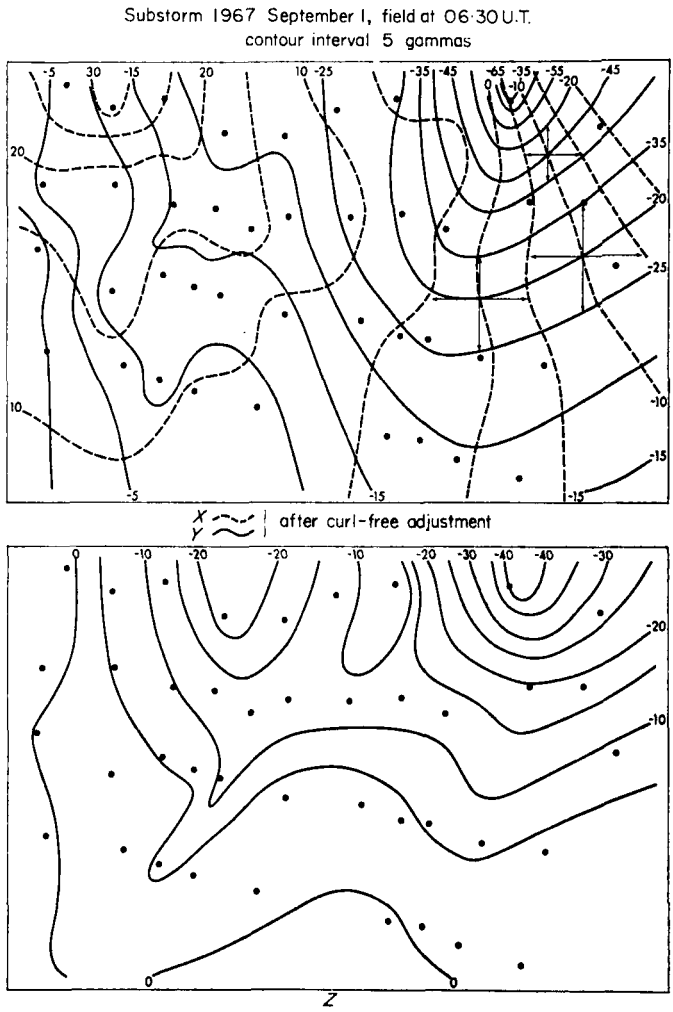

FIG. 2. Maps of three components of instantaneous field at 06·30 U.T.

The separated external fields are in general smooth and the anomalies appear in the internal vertical and eastward fields, Z_i and Y_i. The Z_e field increases northward, as expected, toward the auroral-zone current concentration. Increased southward gradients near the north-east corner of the Z_e map probably reflect edge effects in the separation near a large anomaly near Crawford, Nebraska, which makes the extrapolation of fields very unreliable there. Edge effects may also account for increases in the westward gradients near the western edges of the Z_e map. The east–west gradient of the external field component is generally smooth.

The internal vertical and eastward fields, Z_i and Y_i, show two prominent anomalies. These are no doubt less sharply shown than they might have been without the smoothing effect of averaging field values over 100 km squares. A northward line current would cause a maximum in Y above itself and in Z displaced to the east, and a minimum in Z to the west. The Y_i map of Fig. 3 shows minima along two north–south lines, one along the Wasatch Front which roughly bisects Utah and the other along the Southern Rockies. The Z_i map shows minima somewhat east of those in Y_i. Southward currents under the Wasatch Front and Southern Rockies are indicated.

Separated vertical and eastward fields for 07·15 U.T. are shown in Fig. 4. Strong anomalies appear in the same positions as at 06·30, but reversed in sign. At 07·15 northward currents were flowing under both anomalies. The sign of Y_e was negative (westward) at 06·30 and positive at 07·15. The fields are thus qualitatively consistent with currents induced by an east–west field in north–south striking conductive structures.

The Z_i field at 07·00 (Fig. 5) can be explained with the aid of one further piece of information. Maps of Fourier spectral phases (Reitzel *et al.* 1970) show at all periods studied a phase lag of the Y field of the substorm of September 1 towards the west, of order 10 minutes across the length of the array. The field of the substorm thus swept from east to west across the array with velocity of order 2 km s^{-1}. A possible reason for this, associated with westward growth of the auroral-zone currents, will be discussed elsewhere. Since Y_e changes direction from westward over the whole array at 06·30 to eastward at 07·15, a zero countour of Y_e must have crossed the array between these times. When it did so one would expect the induced currents to reverse their directions, with some phase difference. Whatever the phase difference, the Southern Rockies current should reverse before the Wasatch Front one. For consistency with the fields before and after 07·00, we expect at the transition a northward current under the Southern Rockies and a southward current under the Wasatch Front. These would combine to give a single minimum in Z_i (upward field) between the two currents. This is what the Z_i map at 07·00 shows. The Y_i map reflects the same antiparallel currents. The variograms of Fig. 2 in Reitzel *et al.* (1970) show that Y changes sign near 07·00 U.T., as required.

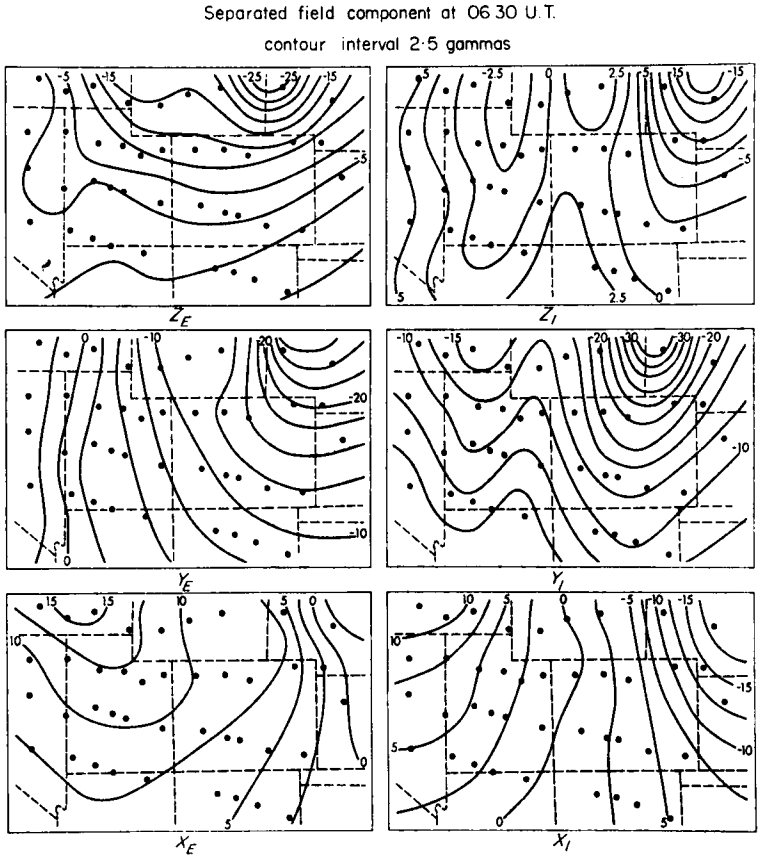

FIG. 3.

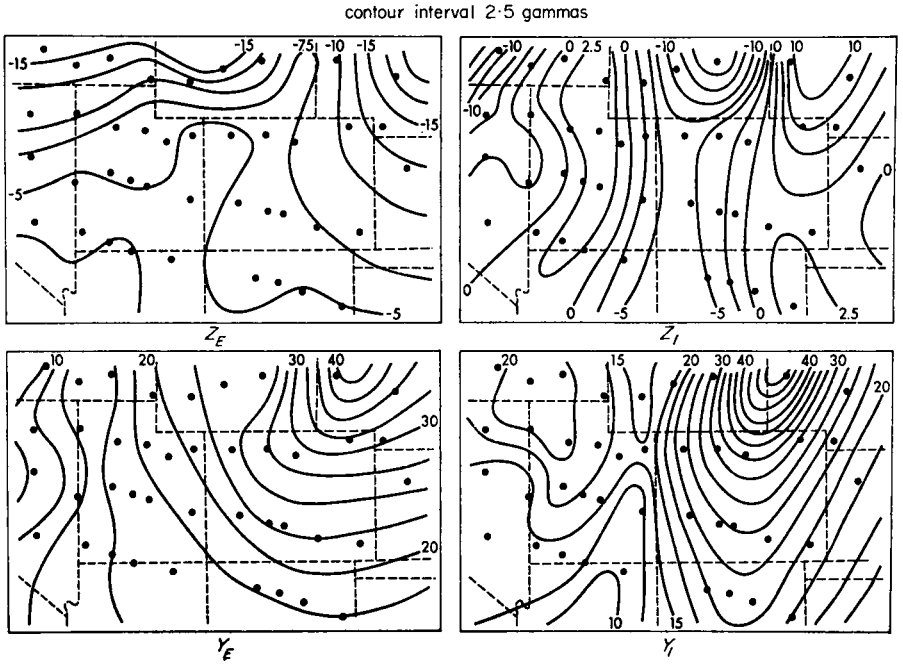

FIG. 4.

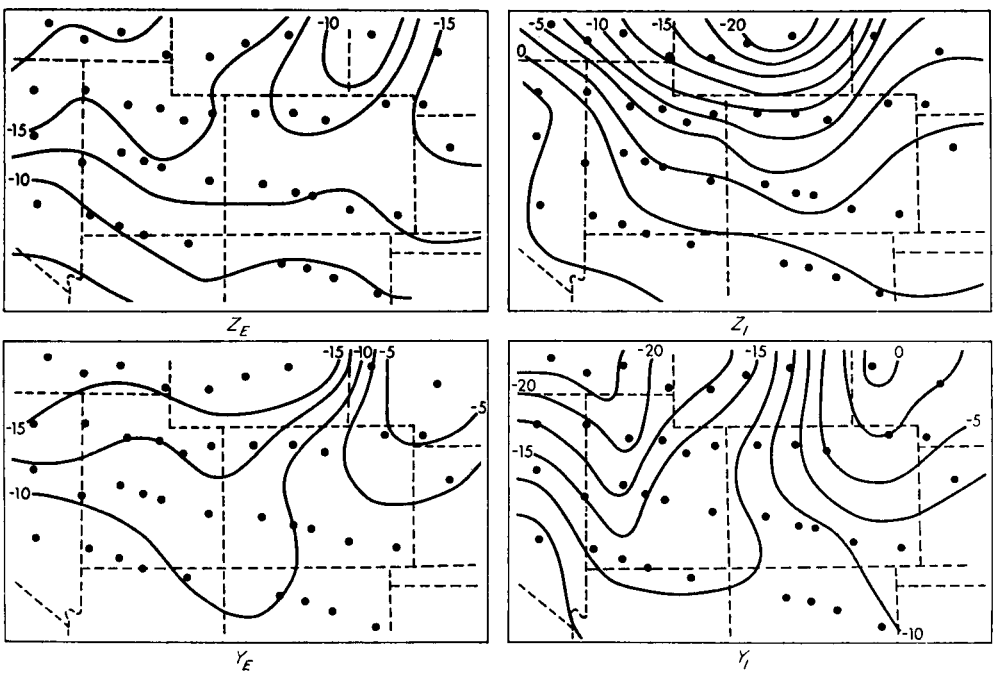

FIG. 5.

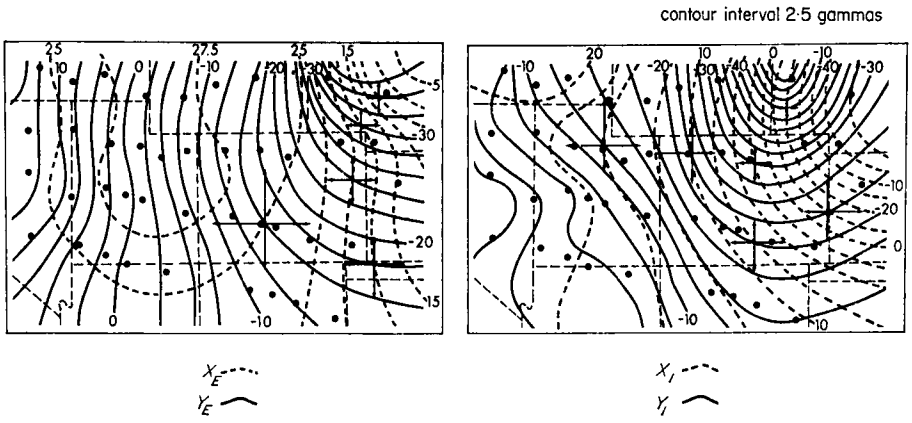

FIG. 6.

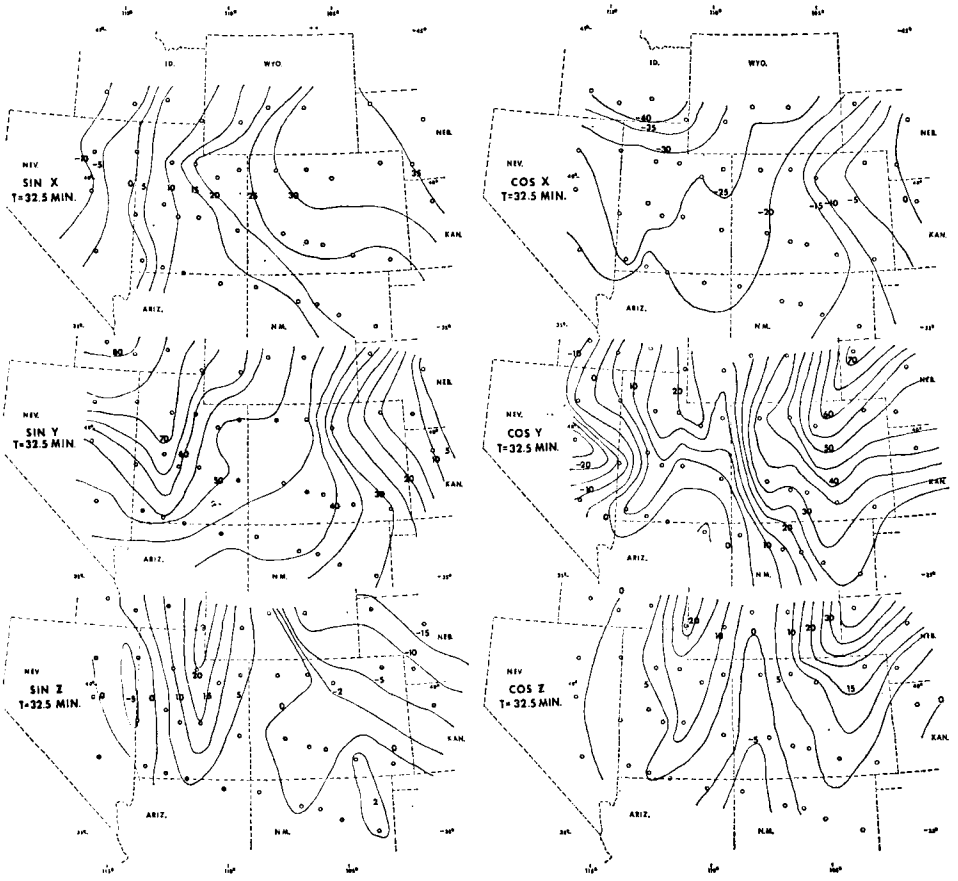

FIG. 7a. Maps of sine and cosine transforms of X, Y and Z at period 32·5 minutes. Units are arbitrary.

The external and internal horizontal fields at 06·45 are superposed in Fig. 6 to show that the separated fields remain curl-free, as they should. It will be seen that a minimum in Y_e coincides with a maximum in X_e, as expected. Instantaneous values of Y_e, Y_i, Z_e and Z_i at nine points along a central east–west profile (not shown) indicate phase leads of the internal fields of order a few minutes. However the phase difference cannot be accurately determined from four points in the time domain.

5. Separated fields in the period domain

Sine and cosine Fourier transforms of the substorm event of 1967 September 1, between 05·00 and 08·30 U.T., have been computed in a manner described elsewhere (Reitzel *et al.* 1970). Contour maps of the sine and cosine transforms are shown in Fig. 7 for the periods 32·5, 50 and 89 minutes. The phase relationships between the magnetic components would be clearer in maps of sine and cosine transforms relative to zero phase of the inducing east–west variation field. With the systematic phase lag of Y to westward already discussed, there is a risk that phase differences other than those due to source effects would be masked if one set the phase of Y to zero at all stations. For this reason the phases relative to 05·00 U.T. have been retained. The anomaly pattern is more accentuated than that in the time

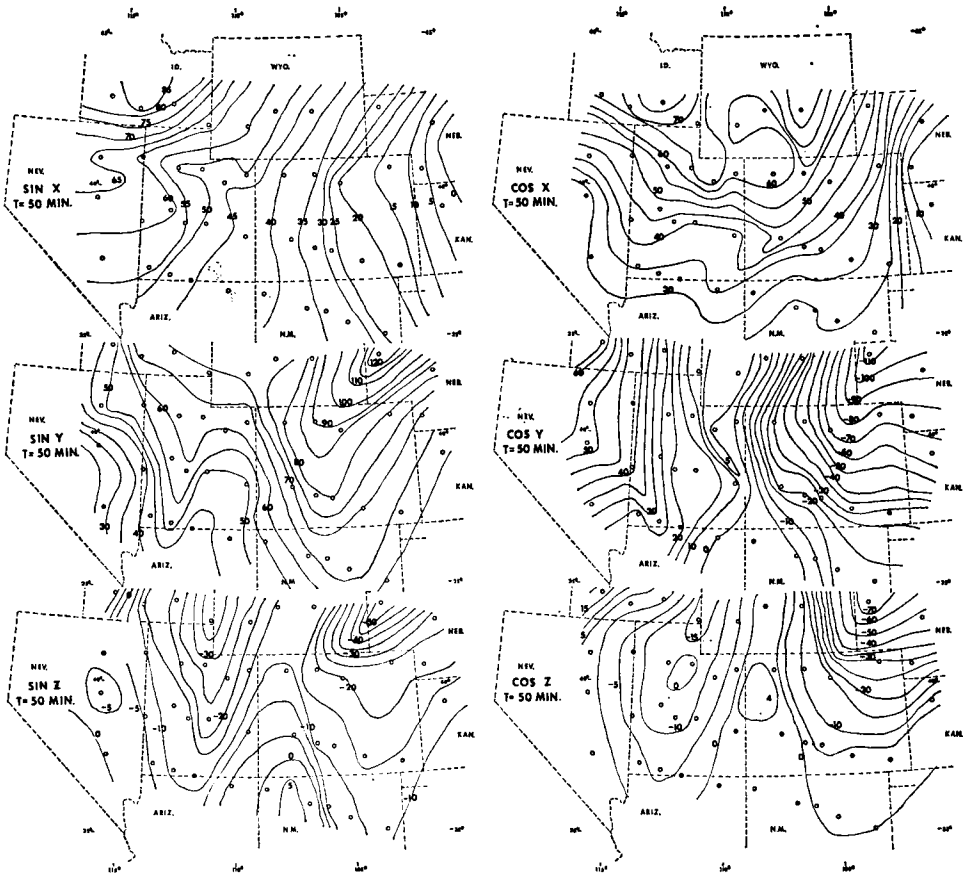

FIG. 7b. Maps of sine and cosine transforms of X, Y and Z at period 50 minutes. Units are arbitrary.

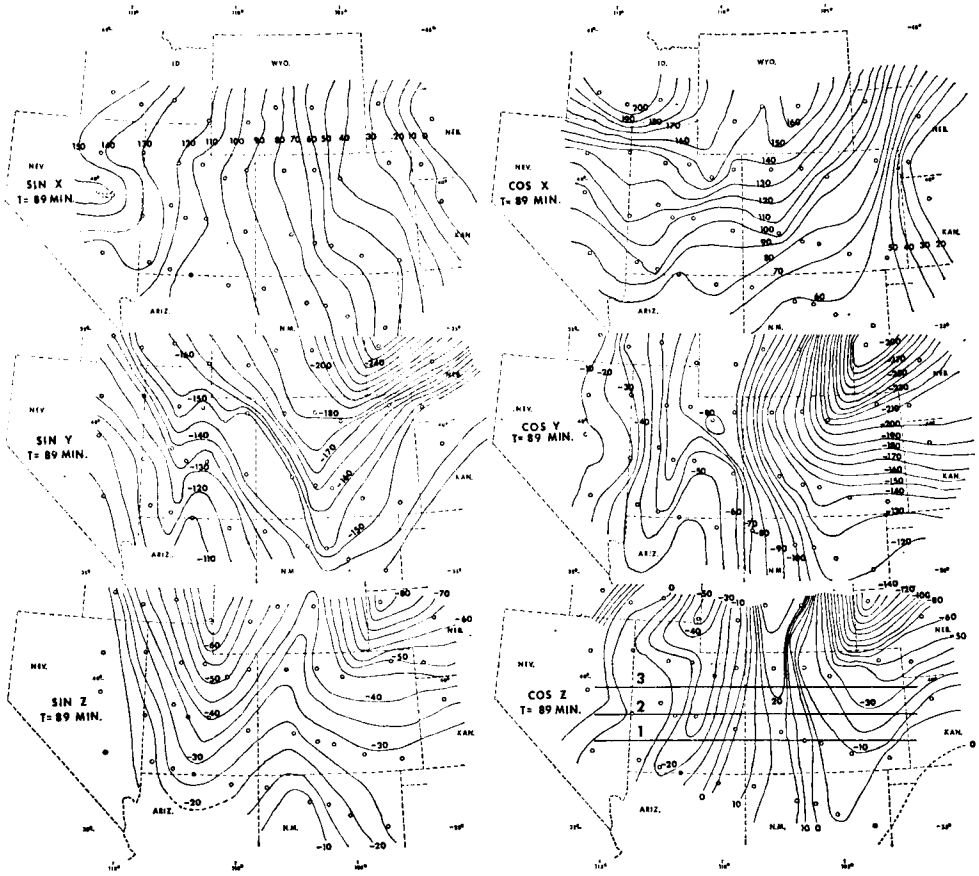

FIG. 7c. Maps of sine and cosine transforms of X, Y and Z at period 89 minutes, showing three profiles used in Fig. 9. Units are arbitrary.

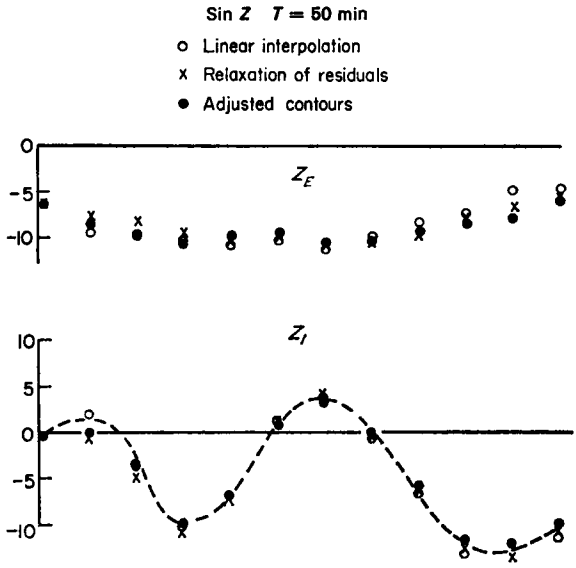

FIG. 8. Separations of Z fields using three interpolation methods for the X and Y fields. Units are arbitrary.

domain, probably because of the removal in the Fourier transformation of slowly-changing field components which do not show the anomalies and effectively dilute the anomaly pattern in the time-domain maps.

A comparison has been made of the effects of three different techniques of interpolation of the horizontal field components, upon the separation of the sine transform coefficients of Z at $T = 50$ minutes. Contour maps of the sine transforms of X and Y at this period were prepared in three ways:

1. By linear interpolation between variometer stations.

2. By drawing a grid of squares 100 km × 100 km on the linearly interpolated map; computing the line integrals along the boundaries of the squares; and relaxing the residual line integrals by the method of Price & Wilkins (1963). Before relaxation the line integrals were generally not zero and the field terms in the residuals were of order 10–20 per cent of the mean values of the horizontal fields in the square.

3. By graphical adjustment of the contours of X and Y to approximate a curl-free field, in the manner discussed in Section 4.

External and internal parts of the sine transforms of Z, separated by the use of the X and Y maps prepared in these three ways, are shown in Fig. 8 for one centrally-located east–west profile. It is clear that anomalous internal Z is quite similar for the three techniques; the results differ only in detail.

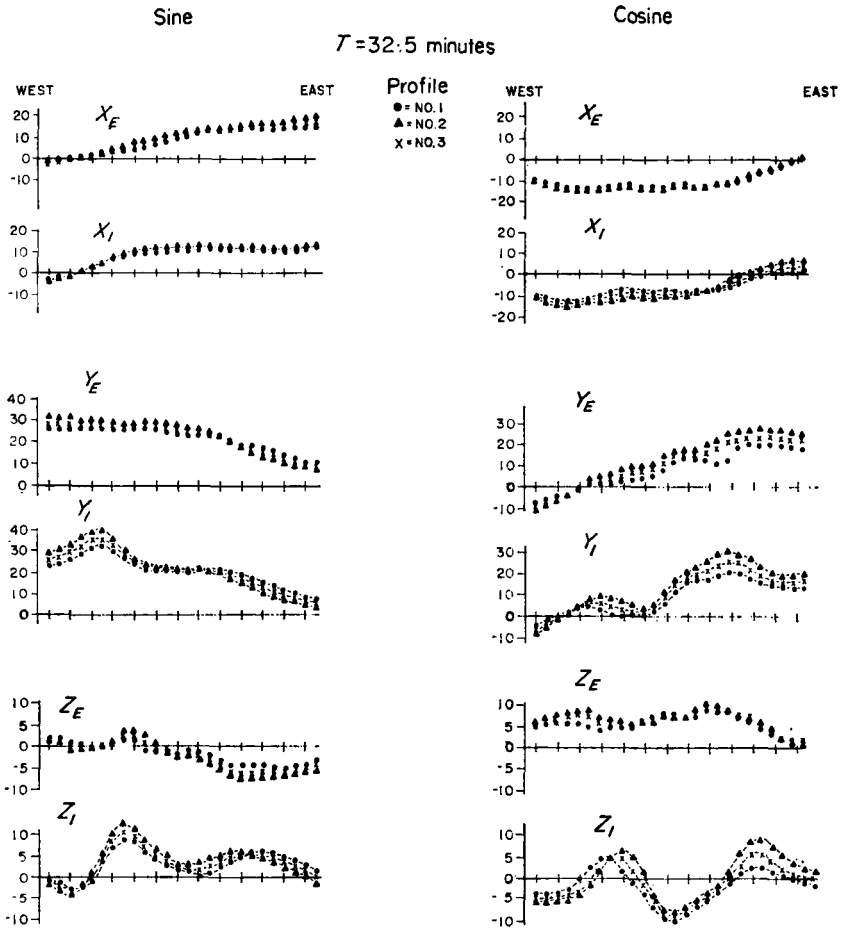

FIG. 9a. Profiles of separated fields for period 32·5 minutes. Units are arbitrary.

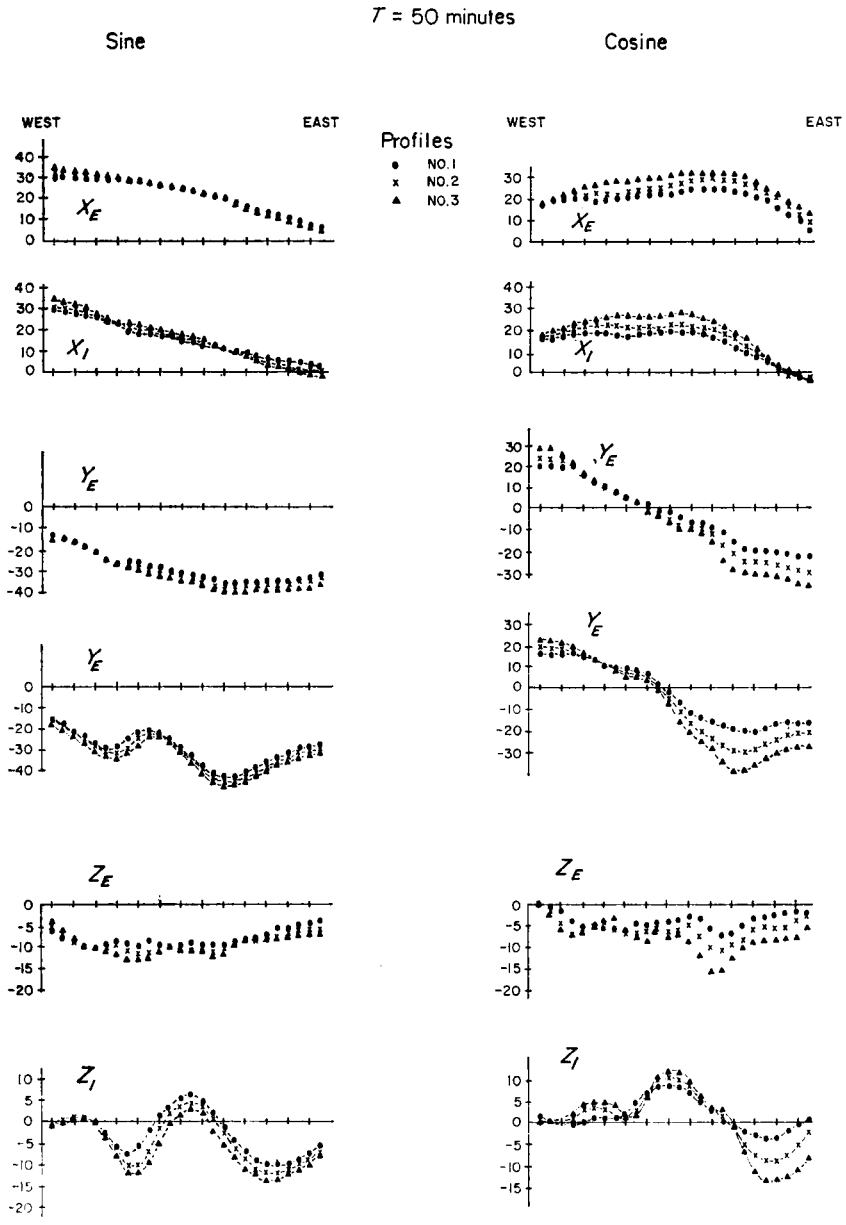

FIG. 9b. Profiles of separated fields for period 50 minutes. Units are arbitrary.

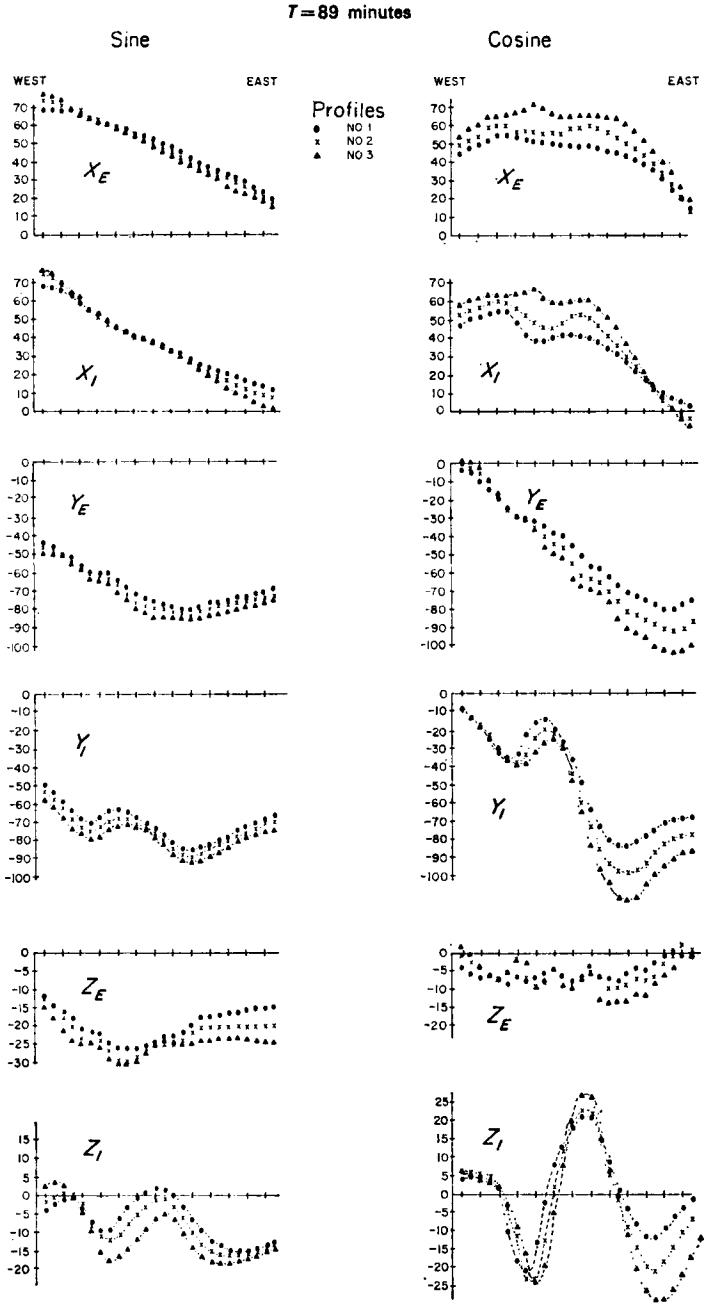

Fig. 9c. Profiles of separated fields for period 89 minutes. Units are arbitrary.

Results of separations in the period domain are shown in Figs 9 and 10. Those for periods 32·5, 50 and 89 minutes, separated in polar co-ordinates as explained above, are shown in Fig. 9 in the form of three centrally-located east–west profiles across the array. This presentation is chosen first because the principal anomalies were already known to strike north–south; and second to minimize edge effects, specially those near the north edge of the array.

To allow comparison of separated fields in the period domain with those in the time domain, results are given in Fig. 10 of separations of Fourier transforms of the substorm field at period 60 minutes. These maps show amplitudes and phases of the external and internal fields intead of the alternative sine and cosine coefficients. Contours near the edges of these maps, in particular the north edge, must, as before, be treated with reserve.

The external horizontal fields are smooth and generally consistent with those of a polar substorm. The Y_e component increases eastward and may be approaching a maximum near the eastern limit of the array. X_e increases toward the west (Fig. 9). Rostoker (1968) has suggested that the field of a polar substorm has a demarcation line where $D = 0$ and H is a maximum for a given geomagnetic latitude. The spatial variations of Y_e and X_e across the array would be as expected for a substorm field whose demarcation line was west of the array through most or all of the time interval integrated in the Fourier transformation. Z_e has no large east–west gradients except local ones which may arise from edge effects or from real local inhomogeneities in the external field.

Each internal field component given by our separation procedure, F_{is}, includes the anomalous internal field F_{ia} related to local conductivity structures, and also some fraction β of the inseparable normal field F_n:

$$F_{is_j} = F_{ia} + \beta F_n. \tag{4}$$

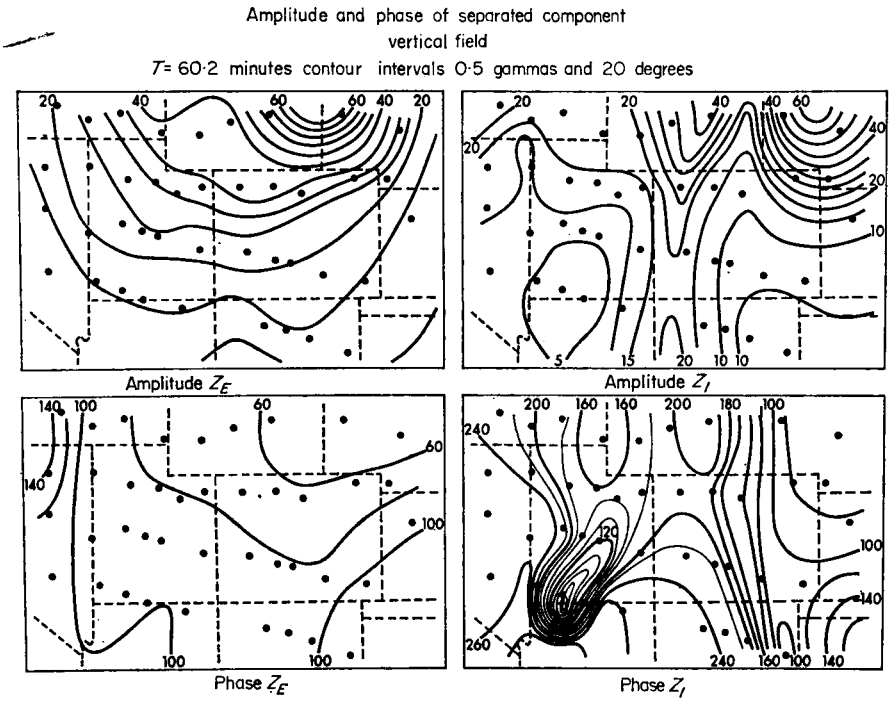

FIG. 10a.

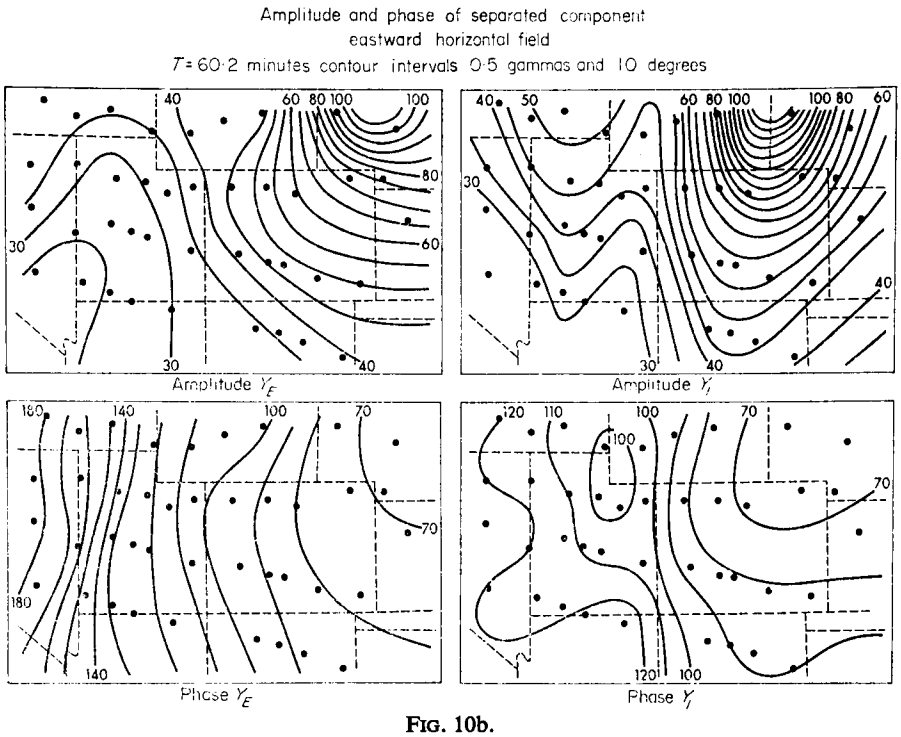

FIG. 10b.

The normal field F_n is that which would exist in the absence of conductive structures, and is the sum (for X and Y) or difference (for Z) of the field F_e of the external currents and the normal internal field F_{in} of currents induced by F_e in the conductive mantle at depths greater than those of the anomalous conductive structures. The external field component given by the separation, then, is

$$F_{es} = (1-\beta)\, F_n. \tag{5}$$

The curves of Fig. 9 and maps of Fig. 10 of F_{is} thus include the smoothly-varying or constant field βF_n. Anomalies of scale lengths less than the array dimensions form part of F_{ia}: indeed it is the size of the array that defines which fields are separable, 'anomalous' internal fields and which are inseparable, 'normal' ones.

Qualitatively the Y_{ia} and Z_{ia} patterns are again indicative of north–south striking currents under the Southern Rockies and Wasatch Front. Maximum gradients in Z_{ia} coincide with maxima in Y_{ia} over these currents. The small anomalies in X_{ia} are consistent with roughly north–south strike of the conductive structures.

Quantitative estimation of the phase differences between normal and anomalous fields, and the approximation of the observed variations by conductivity models, require isolation of the in-phase and out-of-phase (quadrature) components of Y_{ia} and Z_{ia} normalized with respect to the field which induces the anomalous currents. In the plane approximation the conductive mantle at depth becomes a half-space. At a distance outside its plane boundary small compared with the scale-length of the F_e field, F_{in} will be independent of this distance, that is of the depth. Hence the normal field, F_n, at the surface will be the inducing field at a conductive structure above the boundary of the conductive mantle. By (5), $F_n = F_{es}/(1-\beta)$ and the inducing field can be found if β is known. The anomalous internal fields F_{ia} can then be found from (4), and can be normalized with respect to the inducing fields F_n.

For north–south striking structures the inducing field will be the vector sum of Y_n and Z_n. When smoothed to remove local inhomogeneous external fields, Z_{es}

shows only small east–west gradients over the centre of the array (Z_E in Figs 9a, b and c). From equations (1) it is evident that a field with zero east–west gradient makes zero contribution to the difference $Y_e - Y_i$, and that Y_{in} is thus equally divided between Y_{es} and Y_{is}, i.e. $\beta = 0{\cdot}5$. Hence in this case (5) and (4) become

$$\left.\begin{aligned} Y_n &= 2Y_{es} \\ Y_{ia} &= Y_{is} - Y_{es}. \end{aligned}\right\} \quad (6)$$

Deduction of Y_{es} from Y_{is} yields almost equal positive and negative amplitudes of the anomalous internal east–west fields Y_{ia}; the true baseline is indeterminate and depends on the conductivity model chosen to account for the anomaly.

The normal horizontal variation fields X and Y are to first approximation represented by a curl-free plane. For a plane, equations (1) show that Z_n appears in unequal parts in Z_{es} and Z_{is}, such that

$$(Z_n)_{es} - (Z_n)_{is} = \frac{A}{2}\left(\frac{\partial X}{\partial x} + \frac{\partial Y}{\partial y}\right)$$

where A is the radius of the summation window (Section 3). Using (4) and (5),

$$\left.\begin{aligned} Z_{ia} &= Z_{is} - Z_{es} + \frac{A}{2}\left(\frac{\partial X}{\partial x} + \frac{\partial Y}{\partial y}\right) \\ Z_n &= Z - Z_{ia}. \end{aligned}\right\} \quad (7)$$

Hence the anomalous internal vertical field can be isolated and also the normal vertical field. In practice Z_n is small compared with Y_n and only the latter has been used to normalize the anomalous internal vertical and eastward fields. In-phase and out-of-phase components of Z_{ia}/Y_n and Y_{ia}/Y_n are shown in Fig. 11 for one east–west profile at $T = 32{\cdot}5$, 50 and 89 minutes. A point in the Colorado Plateau was arbitrarily given zero value of Y_{ia}/Y_n. Both Y_{ia} and Z_{ia} have been normalized with respect to local Y_n, and therefore are freed from effects of phase of the source field. The interpretation in terms of conductivity models given in the next section is based on the data of Fig. 11.

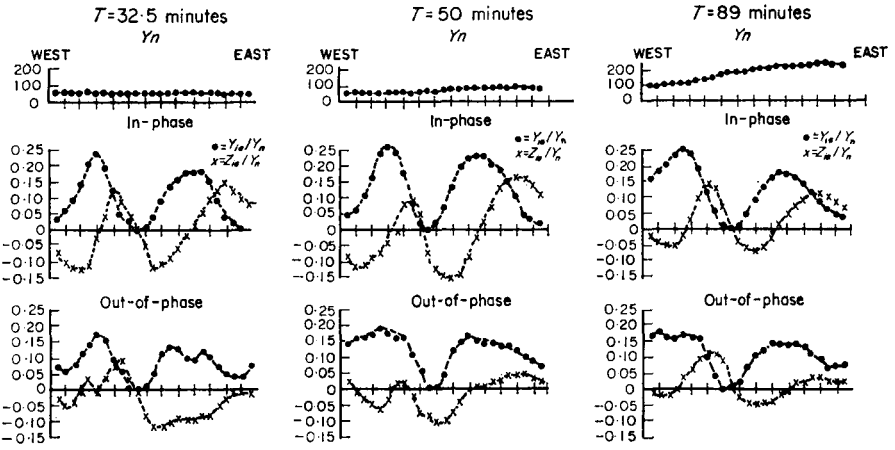

FIG. 11. Normalized anomalous vertical and eastward horizontal fields at three periods.

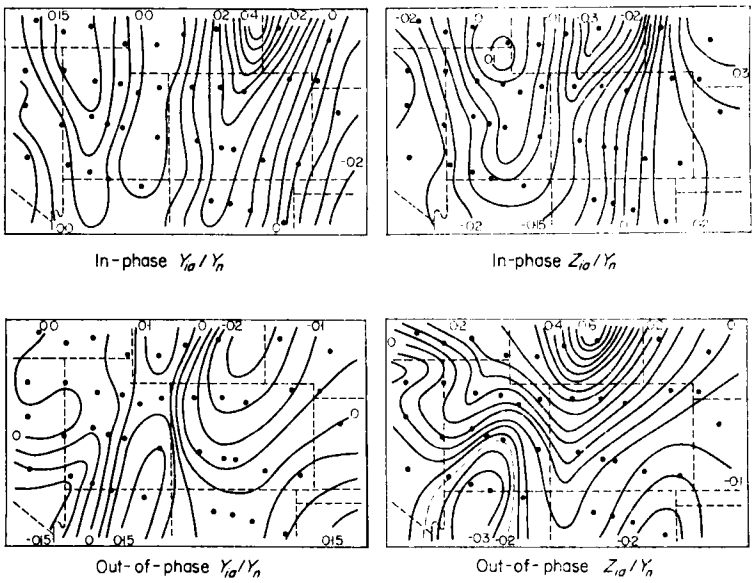

FIG. 12. Normalized anomalous internal fields of substorm at $T = 60$ min. Contour interval = 0·05.

Fig. 12 shows the normalized anomalous fields, Y_{ia}/Y_n and Z_{ia}/Y_n. The in-phase maps show the two north–south currents very clearly as a result of isolation and normalization of their fields. Although edge effects must be present, they do not appear to be severe. Maps such as these may give the best available representation of the anomalous fields. The out-of-phase maps show the north–south currents with complications which may be associated with superficial conductors.

6. Conductive structures: general considerations

The rather wide spacing of variometers in our array and the averaging procedures involved in the separations mean that the normalized anomalous fields shown in Fig. 11 are smoothed: they necessarily fail to show details which a denser array would have shown. However, the existence and rough locations of the two main anomalies were suspected when the array was planned. In consequence, variometers were more closely spaced near extrema of the anomalies than elsewhere. We believe we have enough information of half-widths and locations of the anomalies to justify an interpretation in terms of conductivity models.

The work described in the paper by Reitzel *et al.* (1970) and in this paper has established the presence of approximately two-dimensional north–south striking conductive structures. A single east–west line of more closely spaced stations across these would permit closer study of the structures; for with appropriate inducing fields a two-dimensional separation would suffice. A closely spaced line of variometers will be operated from Kansas to the Pacific for this purpose.

Local anomalies in geomagnetic variations can often be accounted for by conductive structures of one of three types (Schmucker 1964):

1. Anomalies caused by high conductivities in near-surface crustal rocks. These may be related to deep basins of porous sediments saturated with electrolytic solutions. For each superficial conductors the dimensions and resistivity are such that ohmic resistance is more important than inductive reactance. In consequence large phase differences are usually observed between normal and anomalous fields.

2. Isolated cylindrical or spherical conductors in an insulating medium.

3. Undulations in surfaces of equal conductivity in a conducting medium of large extent. Because of the relation between conductivity and temperature this type of model is suitable for deep conductive structures in the Earth. The surfaces of equal conductivity may in fact be isothermal surfaces.

For conductivities and dimensions of upper mantle structures, self-induction controls the currents rather than resistance. In the limit for a large, very highly conducting body the phase difference between the normal and anomalous fields tends to zero.

It will be seen in Fig. 11 that the out-of-phase normalized anomalous field components show generally similar shapes to those of the in-phase field components, though with some disturbance and smaller amplitudes. It is clear, therefore, that most of the quadrature fields are generated by the same deep currents as the in-phase field. Irregular superficial conductivity contrasts may contribute 'noise' superposed on the out-of-phase fields. Estimates of phase differences between Y_n and Y_{ta} or Z_{ta}, from ratios of the in-phase and out-of-phase fields, lie between 25° and 35°. For $T = 60$ minutes the corresponding time lags are 4 to 6 minutes.

The shapes of the anomalies in the in-phase field components show dependence upon period (Fig. 11). In particular the Wasatch Front anomaly is symmetrical for Y and the Z anomaly has nearly equal positive and negative amplitudes at $T = 32{\cdot}5$ and 50 minutes, but both Y and Z become asymmetrical at $T = 89$ minutes. These facts suggest that a symmetrical anomaly, caused by a conductive ridge, may be superposed on an asymmetric anomaly due to a step in the conductive mantle up from the Colorado Plateau to the Basin-and-Range. A structure of this sort had already been suggested (Reitzel *et al.* 1970) from inspection of contour maps of Fourier transform amplitudes and phases of the unseparated fields. The Southern Rockies anomaly remains much more symmetrical as the period increases, though slight asymmetry appears in Z at $T = 89$ minutes. This will be shown to be a result of overlap of the eastern tail of the Wasatch Front anomaly at this period.

Local internal currents should give ratios of (range of Y_{ta})/(range of Z_{ta}) near unity. These ratios for the anomalies of Fig. 11 are given in Table 1, and are near unity within the precision of the analysis except at period 32·5 minutes. At this period the energy in the substorm field is lower and superficial conductors will be relatively more important.

Table 1

			Depth (from half-width) km	
	T	Y_{ta}/Z_{ta}	Line current	Cylinder
Southern Rockies	32·5	0·7	180	370
	50·0	0·9	190	400
	89·0	0·9	200	410
Wasatch Front	32·5	1·0	110	230
	50·0	1·2	125	260
	89·0	1·2		

7. Conductive structures: models

To obtain depth estimates and to approximate the observed in-phase anomalous fields, line currents and upheavals in a perfect conducter will be used as models. For the observed phase differences of order 30 degrees a perfect conductor is a reasonable first approximation. Once limits have been set on the dimensions of

an upheaval, the conductivity can be estimated from the phase differences. The usual simplifying assumptions are made of a horizontal normal field of scale-length large compared with the anomalous structures. These assumptions hold in good approximation.

Schmucker (1959) considered the variation anomaly due to a surface current of variable density flowing along the strike of undulations on a perfect conductor. Line currents and cylindrical conductors are two approximations to such undulations. From either, one can obtain depth estimates from half-widths of the horizontal-field anomaly or from the distance between peaks of the Z anomaly. The response of an undulating perfect conductor depends on its depth and on the amplitude and wavelength of the undulations. The line current model is the limiting case of an undulation with zero wavelength and infinite amplitude (Schmucker 1959), that is a current along the edge of a thin vertical plate. This model was considered by Bartels (1954) for the North German anomaly. It follows that a depth estimate on a line current model gives a maximum depth to the top of the conductor. Depth estimates of this kind are given in Table 1: they are close to 190 km for the Southern Rockies and 120 km for the Wasatch Front. These must be considered rough estimates, as the observed fields are asymmetric, especially at $T = 89$ minutes.

A variation anomaly which can be modelled with a line current can also be produced by infinitely many current configurations at smaller depths. This underlines the relative nature of the geomagnetic deep sounding method, caused by the limited dimensions of the variometer array. The phase difference as function of period depends on the shape, dimensions and conductivity of the structure, and absolute parameters cannot be gained without the aid of a reference normal conductivity section at a distance from the anomaly. In principle such a reference section can be secured from suitable magnetotelluric observations. Heat flow data, and the inability of superficial conductors to account for observed phase differences or for the anomalies in the daily variation field (Reitzel *et al.* 1970), lead us to relate our results to a temperature anomaly in the upper mantle.

Two-dimensional anomalous fields can often be approximated by conformal mapping of a perfectly conducting half-space into simple structures on its surface (Schmucker 1964). Semi-circular and step structures will suffice for our anomalies. A mapping function $w(z) = u+iv$ $(z = x+iy)$ is chosen which maps the surface, $y = 0$, of the half-space into the specified structure. This function is then used to map the equipotentials (x = constant) and field lines (y = constant) for a grid of points outside the conductor. The anomalous field components are then obtained from the potential gradients. For a semi-circular upheaval of radius R the mapping function is

$$w(z) = \frac{R}{2}\left(z+\sqrt{(z^2-4)}\right). \tag{8}$$

(Schmucker 1969). For a step structure of height h

$$w(z) = \frac{h}{\pi}\left(\sqrt{(z^2-1)}+\cosh^{-1} z\right) \tag{9}$$

(Churchill 1960, p. 291).

A semi-circular upheaval gives the field of a two-dimensional dipole superposed on a uniform horizontal field. The corresponding current configuration would consist of two linear currents of opposite polarities. Such a current system has no physical reality in a mantle upheaval. It must be remembered, however, that the anomalous field is observed in the presence of much larger normal fields. Induction in the upheaval produces a current concentration along its crest and a reduction of

the normal current at either side. These current reductions can be regarded as equivalent to a return current along their geometrical centre, under the forward current.

The observed anomaly fields have been approximated by semi-circular upheavals and a step in the surface of a perfectly conducting half-space. The in-phase fields at $T = 89$ minutes were chosen as the field has largest energy at this period and errors in the separation analysis will be least. For the Southern Rockies, initial depth estimates to the top of the conductor (line current model) and to the depth z of the unperturbed conductor (two-dimensional dipole model) were taken from half-widths of the Y_{ia} anomaly (Table 1). This gave an initial estimate of the radius R. As expected, the depth estimates increase somewhat with period, reflecting the increased penetration of the variation fields of longer period. The small range of the estimates suggests a highly-conducting medium. The parameters z and R were then adjusted to fit the observed Z and Y anomalies.

In this way the vertical-field maximum east of the Southern Rockies was fitted by a semi-circular upheaval ($R = 150$ km, $z = 360$ km) (Fig. 13a). The vertical field for this structure has substantial amplitudes at the Wasatch Front, so that the baseline of the Wasatch Front anomaly must be corrected. This increases the asymmetry of the vertical field anomaly at the Wasatch Front. The difference between the observed field and that of the Southern Rockies model was next approximated by a step ($h = 110$ km) under the Wasatch Front (Fig. 13b). The residual field was then fitted by a semi-circular upheaval ($R = 100$ km, $z = 250$ km) under the Wasatch fault belt on top of the step (Fig. 13c). The fit to the observed vertical field is not perfect for the central Colorado Plateau, where smaller Z amplitudes are required. The low station density in this area and the simplifying assumptions used make it unjustifiable to elaborate the model further.

A similar model was fitted in corresponding stages to the horizontal anomalous field (Fig. 14). The model agrees rather well with that for the vertical field. For the periods 32·5 and 50 minutes, correction for the vertical anomaly field of the Southern Rockies upheaval makes the Wasatch Front anomaly asymmetric. However, the asymmetry will be less than at $T = 89$ minutes, giving a smaller step height and therefore a more symmetrical vertical field over the Southern Rockies.

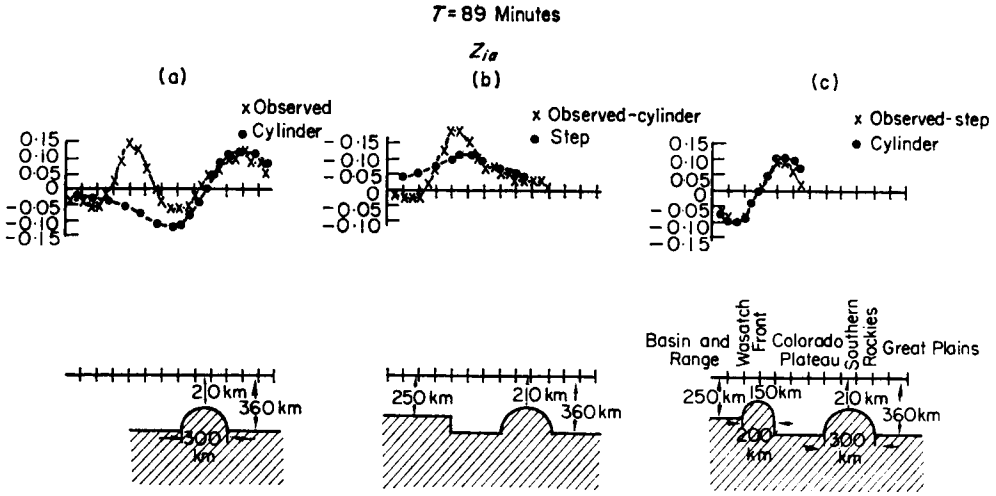

FIG. 13. Conductivity model approximating the vertical anomaly field.

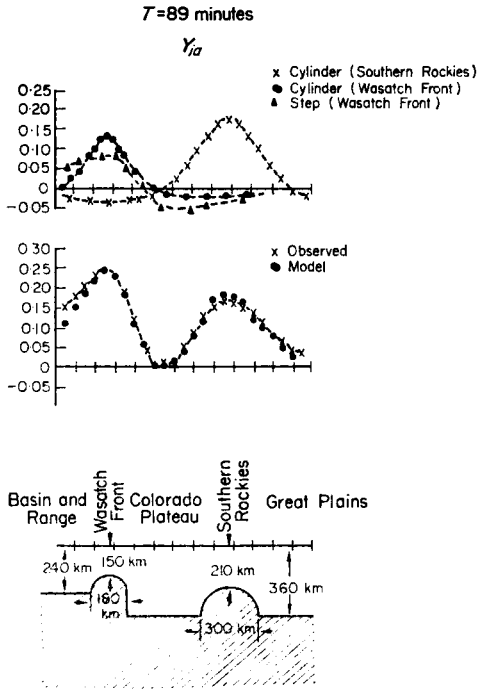

FIG. 14. Conductivity model approximating the eastward horizontal anomaly field.

In modelling both the vertical and horizontal anomaly fields, the step and semi-cylinder at the Wasatch Front have been superposed. This is strictly incorrect, as each structure modifies the field which induces current in the other. The error introduced will be greatest at the Wasatch Front and is believed to be smaller than the uncertainty in the observed anomalies.

8. Conductivity and temperature

To examine a possible relation between the conductivity model and isothermal surfaces in the upper mantle, we first estimate the real conductivity in the model structures from phase differences between the normal and anomalous fields. The calculation is most convenient for the semi-circular upheaval under the Southern Rockies. Such an upheaval has the same response as an isolated cylinder (Kertz 1960; Rikitake & Whitham 1964). The relevant induction parameter is $c = r\sqrt{(4\pi\omega\sigma)}$. The constant c can be found from the relative magnitudes of the in-phase and out-of-phase fields. The radius r of the cylinder can be obtained from the maximum amplitude of the anomalous horizontal field $W = Y_{ia}/Y_n$ (Schmucker 1959) as

$$r = z\sqrt{(W/f)}$$

where f is the fraction of the dipole moment of a perfectly conducting cylinder, and can be obtained from the phase differences. For the Southern Rockies $z = 360$ km, $W = 0{\cdot}175$ and $f = 0{\cdot}6$, so that $r = 200$ km. With $c = 3{\cdot}5$ e.m.u. corresponding to phase angle 30°, we find for the conductivity $\sigma = 2{\cdot}10^{-12}$ e.m.u.

Experimental data on the relation between electrical conductivity and temperature in upper-mantle materials show considerable dependence on the composition assumed, and require extrapolation to reach the conductivity estimate just given. For reasonable fayalite concentrations the temperature will lie in the vicinity of

1500°C (Hamilton 1965). Clarke & Ringwood (1964) give this temperature at depth 350 km under a continental shield. This is consistent with the depth to the unperturbed conductor under the Great Plains in our model.

The general correspondence between our induction anomalies and the heat-flow distribution has been pointed out elsewhere (Reitzel *et al.* 1970). Our conductivity model is consistent with the observed similar values of heat flow over the Southern Rockies and in the Basin-and-Range (Roy & Blackwell, in preparation), because the smaller depth to the Southern Rockies structure will be offset by its limited width.

It should be noted that our model gives the same depth to the highly-conductive mantle under the Colorado Plateau as under the Great Plains. A step structure near the Southern Rockies is definitely excluded. Higher heat-flow values may be expected in the Colorado Plateau, however, as it lies between two heat sources.

Acknowledgments

We are indebted to Dr John S. Reitzel for helpful discussions. The University of Alberta group was supported by grants from the Defence Research Board and National Research Council of Canada. The University of Texas at Dallas group was supported by National Science Foundation grant number GA647.

H. Porath:
University of Texas at Dallas.

D. W. Oldenburg and D. I. Gough:
University of Alberta,
Edmonton, Canada.

References

Bartels, J., 1954. Erdmagnetisch erschliessbare lokale Inhomogenitäten der elektrischen Leitfähigkeit im Untergrund, Nachr. Akad. Wiss. Göttingen, II. *Math. Phys. Kl.*, 2a, 95–100.

Chapman, S. & Bartels, J., 1940. *Geomagnetism*, Oxford University Press, London, 1049 pp.

Churchill, R. V., 1960. *Complex variables and applications*, McGraw Hill, New York, 291 pp.

Clarke, S. P. & Ringwood, A. E., 1964. Density distribution and constitution of mantle, *Rev. Geophys.*, **2**, 35–88.

Gough, D. I. & Reitzel, J. S., 1967. A portable three-component magnetic variometer, *J. Geomagn. Geoelect.*, **19**, 203–215.

Hamilton, R. M., 1965. Temperature variation at constant pressure of the electrical conductivity of periclase and olivine, *J. geophys. Res.*, **70**, 5679–5692.

Hartmann, Q., 1963. Behandlung lokaler erdmagnetischer Felder als Randwertaufgabe der Potentialtheorie, Abhandl. Akad. Wiss. Göttingen, *Math. Phys. Kl., Beitr. I. G. J.*, **9**, 1–50.

Kertz, G., 1960. Leitungsfähiger Zylinder im transversalen magnetischen Wechselfeld, Gerland's *Beitr. Geophys.*, **69**, 4–28.

Price, A. T. & Wilkins, G. A., 1963. New methods of analysis of geomagnetic fields and their application to the *Sq* field of 1932–1933, *Phil. Trans. R. Soc. London, Ser. A*, **256**, 31–98.

Reitzel, J. S., Gough, D. I., Porath, H. & Anderson, C. W., 1970. Geomagnetic deep sounding and upper mantle structure in the western United States, *Geophys. J. R. astr. Soc.*, **19**, 213–235.

Rikitake, T., 1950. Electromagnetic induction within the Earth and its relation to the electrical state of the Earth's interior, 1, *Bull. Earthquake Res. Inst.*, Tokyo Univ., **28,** 45–100.

Rikitake, T. & Whitham, K., 1964. Interpretation of the Alert anomaly in geomagnetic variations, *Can. J. Earth Sci.*, **1,** 35–62.

Rostoker, G., 1968. Macrostructure of geomagnetic bays, *J. geophys. Res.*, **73,** 4217–4229.

Schmucker, U., 1959. Erdmagnetische Tiefensondierung in Deutschland 1957–1959: Magnetogramme und erste Auswertung, Abhandl. Akad. Wiss. Göttingen, *Math. Phys. Kl., Beitr. I. G. J.*, **5,** 1–51.

Schmucker, U., 1964. Anomalies of geomagnetic variations in the Southwestern United States, *J. Geomagn. Geoelect.*, **15,** 193–221.

Schmucker, U. (1969, to be published). Anomalies of geomagnetic variations in the Southwestern United States, Monograph Scripps Inst. Oceanography.

Siebert, M. & Kertz, W., 1957. Zur Zerlegung eines lokalen erdmagnetischen Feldes in äusseren und inneren Anteil, Nachr. Akad. Wiss. Göttingen, II, *Math. Phys. Kl.*, 87–112.

Vestine, E. H., 1941. On the analysis of surface magnetic fields by integrals, *Terr. Mag. Atmos. Electr.*, **46,** 27–41.

Weaver, J. T., 1963. On the separation of local geomagnetic fields into external and internal parts, *J. geophys. Res.*, **29,** 29–36.

Wiese, H., 1965. Geomagnetische Tiefentellurik, Deutsche Akad. Wiss. Berlin, *Geomagn. Inst. Potsdam, Abh.*, **36,** 1–146.